Contents lists available at ScienceDirect

Transactions of Nonferrous Metals Society of China

36(2026) 203−217

www.tnmsc.cn

Numerical model for rapid prediction of temperature field, mushy zone and grain size in heating−cooling combined mold (HCCM) horizontal continuous casting of C70250 alloy plates

Ling-hui MENG [a,b], Fan ZHAO [a,b,*], Dong LIU [c], Chang-jian LU [c], Yan-bin JIANG [d,e], Xin-hua LIU [c,f,**]

[a] Key Laboratory for Advanced Materials Processing (MOE), Institute for Advanced Materials and Technology, University of Science and Technology Beijing, Beijing 100083, China;

[b] Beijing Laboratory of Metallic Materials and Processing for Modern Transportation, Institute for Advanced Materials and Technology, University of Science and Technology Beijing, Beijing 100083, China;

[c] Institute of Materials Genome Engineering, Henan Academy of Sciences, Zhengzhou 450046, China;

[d] School of Materials Science and Engineering, Central South University, Changsha 410083, China;

[e] State Key Laboratory of Powder Metallurgy, Central South University, Changsha 410083, China;

[f] Beijing Advanced Innovation Center for Materials Genome Engineering, University of Science and Technology Beijing, Beijing 100083, China

Abstract: Machine learning-assisted methods for rapid and accurate prediction of temperature field, mushy zone, and grain size were proposed for the heating−cooling combined mold (HCCM) horizontal continuous casting of C70250 alloy plates. First, finite element simulations of casting processes were carried out with various parameters to build a dataset. Subsequently, different machine learning algorithms were employed to achieve high precision in predicting temperature fields, mushy zone locations, mushy zone inclination angle, and billet grain size. Finally, the process parameters were quickly optimized using a strategy consisting of random generation, prediction, and screening, allowing the mushy zone to be controlled to the desired target. The optimized parameters are 1234 °C for heating mold temperature, 47 mm/min for casting speed, and 10 L/min for cooling water flow rate. The optimized mushy zone is located in the middle of the second heat insulation section and has an inclination angle of roughly 7°.

Keywords: Cu alloy; numerical simulation; machine learning; prediction model; process optimization

1 Introduction

In recent years, precipitation-strengthened Cu−Ni−Si alloys exemplified by C70250 have been widely used in high-end electronics such as connectors and integrated circuit lead frames due to their excellent strength and electrical conductivity [1−3]. Cu−Ni−Si alloy billets are generally produced by a traditional process of vertical semi-continuous casting, resulting in high material loss, high energy consumption, and low production efficiency in the subsequent milling, hot rolling, and pickling processes for obtaining strips [4−6]. To solve the above-mentioned problem, a novel process named heating−cooling combined mold (HCCM) horizontal continuous casting was devised by XIE [7] to manufacture Cu−Ni−Si alloy billets with superior surface quality and columnar grains along the continuous casting direction [8]. Billets

Corresponding author: *Fan ZHAO, Tel: +86-10-62332253, E-mail: zhaofan@ustb.edu.cn;
**Xin-hua LIU, Tel: +86-10-62332253, E-mail: liuxinhua18@163.com

https://doi.org/10.1016/S1003-6326(25)66958-5

Received 9 April 2024; accepted 11 December 2024

produced by this method have excellent cold deformation ability and can be directly cold-rolled into strips with no or minimal surface milling [9,10]. However, the control difficulty of HCCM continuous casting process is relatively high. Precisely controlling the temperature field and mushy zone is key to improving the billet quality and obtaining the required grain structure. This requires a comprehensive understanding and regulation of various continuous casting process parameters.

Technological advancements in computing, such as artificial intelligence and digital twin, have pushed material processing toward automation and intelligence [11]. Establishing a rapid and accurate prediction model is essential for achieving rapid optimization and real-time control of process parameters [12]. In recent years, many researchers have developed prediction models for material processing by combining numerical simulation with machine learning, achieving notable progress. DONG et al [13] developed a neural network model to predict the shrinkage of typical blade structures based on data obtained from simulations and experiments. The model demonstrated relatively high prediction accuracy and effectiveness in forecasting the shrinkage of standard hollow thin-walled castings. HÜRKAMP et al [14] created a surrogate model using model reduction techniques and machine learning algorithms to approximate any simulation solution for the in-mold assembly. This surrogate model allows for the rapid and accurate prediction of bond strength. SUN et al [15] investigated the grain growth behavior in dual-phase (DP) steel using Monte Carlo simulation and employed machine learning techniques to perform a sensitivity analysis on the influencing parameters. The primary factors were chosen to facilitate a better understanding of the grain growth process of DP steel. WANG et al [16] introduced a data-driven framework that integrates numerical simulation with the radial basis function optimization method to regulate dimensional accuracy in ring-to-ring casting. Optimized results were found to be in good agreement with practical outcomes. The findings above suggest that one way to overcome the difficulties of acquiring experimental data is to use simulation computing to build foundational datasets for machine learning models.

Based on the foregoing, this study investigated the numerical prediction modeling of the HCCM horizontal continuous casting process for the C70250 alloy. It is believed that the results obtained could provide a basis for digital twin modeling and intelligent control of the HCCM horizontal continuous casting process.

2 Experimental

This study involved simulating the HCCM horizontal continuous casting process with various process parameters to acquire data on the temperature field, mushy zone, and grain size. Subsequently, machine learning models were developed based on the simulation data to enable the rapid prediction of the temperature field, mushy zone, and grain size. Additionally, the impact of process parameters on casting control targets was analyzed using the Shapley Additive Explanations (SHAP) method. Finally, the process parameters were quickly optimized to achieve the desired mushy zone with the help of the prediction model.

2.1 Principle of HCCM horizontal continuous casting

Figure 1 illustrates the schematic diagram of the HCCM horizontal continuous casting, comprising a heating mold and a cooling mold. The heating mold is heated using an induction heating device, while the cooling mold is cooled using a water-cooled copper jacket. By precisely regulating the solidification interface in the transition region between the heating and cooling molds, a significant temperature gradient can be achieved along the casting direction, particularly in the liquid phase near the solid−liquid interface. This temperature gradient facilitates the formation of columnar grains along the casting direction [17].

The main process parameters of the HCCM horizontal continuous casting include heating mold temperature measured by the thermocouple 9 in Fig. 1, drawing speed controlled by the traction device, and cooling water flow rate of the water-cooled copper jacket. These process parameters are the primary variables employed in the simulation and machine learning of this study.

2.2 Finite element simulation and dataset construction

The ProCAST software was used for the finite

element simulation of the continuous casting process. As shown in Fig. 2, a 1/4 finite element model was established according to the actual size of the production enterprise. The total width and thickness of the mold are 711 and 82 mm, respectively. The length of the heating mold section is 76 mm. In front of and behind it are the insulation sections with lengths of 75 and 49 mm, respectively. The length of the cooling mold section is 276.5 mm. After the cooling mold section, the copper billet leaves the mold and enters the air cooling section. The billet is 650 mm wide and 18 mm thick. Tetrahedral elements with a side length of 2 mm were used to mesh the model.

The C70250 alloy used for the simulation and industrial experiment has a chemical composition (wt.%) of Cu−3.2Ni−0.7Si. The material data for the graphite mold were obtained from the ProCAST software database. The copper liquid inlet was set at a constant temperature of 1260 °C. The outside surface of the heat insulation section was set in adiabatic condition. The coefficients of the cooling

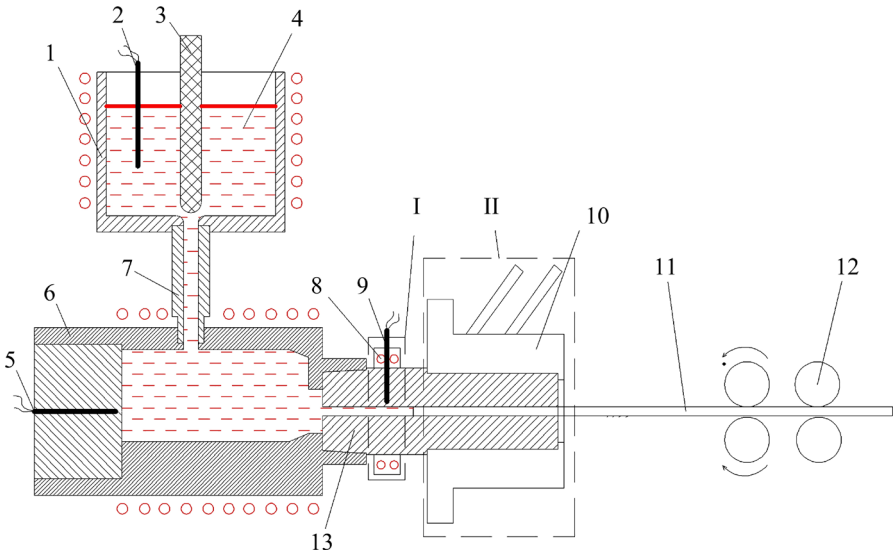

Fig. 1 Schematic diagram of HCCM horizontal continuous casting [17]: 1−Melting crucible; 2,5,9−Thermocouple; 3−Stopper; 4−Alloy melt; 6−Holding crucible; 7−Diversion pipe; 8−Mold heating device; 10−Water-cooled copper jacket; 11−Alloy billet; 12−Traction device; 13−Mold; I−Heating mold section; II−Cooling mold section

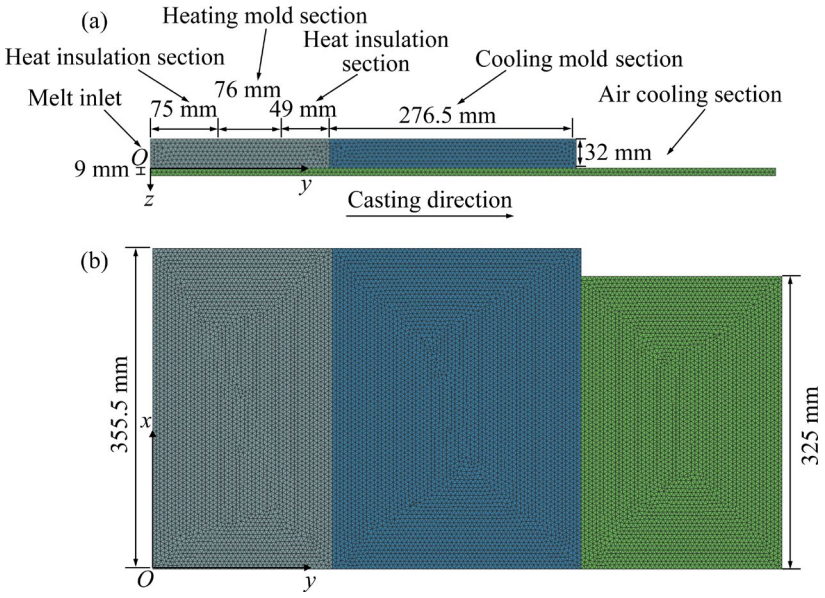

Fig. 2 1/4 model used for finite element simulation of copper alloy plate: (a) View from transverse direction; (b) View from normal direction

mold outside surface were 2000, 4000, and 6000 $W·m^{-2}·K^{-1}$, corresponding to cooling water flow rates of 5, 10, and 15 L/min, respectively. The surface of the copper billet that had moved out of the mold was set in an air cooling condition. The coefficient of air cooling was 30 $W·m^{-2}·K^{-1}$. The heat transfer coefficient between the copper liquid and the mold was 10000 $W·m^{-2}·K^{-1}$. The copper alloy could shrink in volume during solidification, creating an air gap between the plate billet and the mold. Therefore, it is necessary to calculate the air gap width at different temperatures to determine the dynamic heat transfer coefficient between the plate billet and the mold [18]. By combining the solidification shrinkage formula with the measured actual dimensions of the copper plate at the exit of the crystallizer, an air gap width closer to the actual solidification conditions was calculated. The width of the air gap is calculated as follows:

$$\Delta L=\alpha\cdot l\cdot\Delta T \tag{1}$$

where ΔL is the linear dimension of shrinkage, m; α is the linear shrinkage coefficient, K^{-1}; l is the linear dimension before shrinkage, m; ΔT is the temperature change of surface, K. The α value of C70250 used in this research is $17.6\times10^{-6}\,K^{-1}$. The width of the air gap is half of the shrinkage dimension. After obtaining the width of the air gap at different temperatures, the heat transfer coefficient between the copper alloy plate and mold can be calculated by the following equation:

$$h=\lambda/d \tag{2}$$

where h is the heat transfer coefficient, $W·m^{-2}·K^{-1}$; λ is the thermal conductivity of air, $W·m^{-1}·K^{-1}$; d is the air gap width, m. The calculated dynamic heat transfer coefficients are given in Table 1.

The simulation of the temperature field depends on the following heat flow differential equation [19]:

$$\rho c_p\left(\frac{\partial T}{\partial t}\right)=\lambda\left(\frac{\partial^2 T}{\partial x^2}+\frac{\partial^2 T}{\partial y^2}+\frac{\partial^2 T}{\partial z^2}\right)+L\frac{\partial f_s}{\partial t} \tag{3}$$

where ρ is the density, kg/m^3; c_p is the specific heat capacity at constant pressure, $J·kg·K^{-1}$; T is the thermodynamic temperature, K; t is the time, s; L is the latent heat of crystallization, $J·kg^{-1}$; f_s is the solid fraction. With the input of elemental content, the thermodynamic data of the C70250 alloy can be calculated by the simulation software to obtain the solidification fraction versus temperature curve. Then, based on the temperature field simulation results, the coordinate values of the start and end locations of the mushy zone can be calculated.

Table 1 Calculation results of air gap width (d), air thermal conductivity (λ), and heat transfer coefficient between Cu alloy and mold (h) at different Cu alloy temperatures

Cu alloy temperature/K	d/mm	λ/ ($W·m^{-1}·K^{-1}$)	h/ ($W·m^{-2}·K^{-1}$)
303	0.350	0.0267	76.3
323	0.350	0.0283	80.86
373	0.343	0.0321	93.59
573	0.312	0.0461	147.76
773	0.231	0.0575	248.92
973	0.151	0.0671	444.37
1073	0.110	0.0717	649.95
1173	0.07	0.0763	1090
1273	0.03	0.0808	2693.3
1323	0.01	0.0830	8300
1373	0	0.0856	10000

The cellular automaton and finite element (CAFE) method was used to simulate the grain microstructure after solidification [20]. Integrating the discrete spatial modeling of cellular automaton with the continuous physical process simulations of finite element methods, CAFE is a powerful tool for accurately modeling and analyzing the dynamics of grain growth. In the simulation, the contact surfaces between the Cu alloy and the mold were set in surface nucleation conditions, with the mean supercooling degree, supercooling degree standard deviation, and maximum density of the surface nucleation set to be 10 K, 1 K, and $1\times10^8\,m^{-2}$, respectively. The Cu interior was set in volume nucleation conditions, with the mean supercooling degree, supercooling degree standard deviation, and maximum density of the volume nucleation set to be 10 K, 2 K, and $1\times10^7\,m^{-2}$, respectively. First, the initial simulation parameters were selected according to the literature, and the simulation results of grain size and grain inclination angle were compared with the experimental results under different process parameters. Subsequently, the simulation parameters were adjusted continuously until the simulation results matched the experimental results.

With the help of finite element simulation, the data on temperature field, mushy zone, and grain size were obtained. Sixty sets of different process parameters were used for the finite element simulation, including drawing speed, heating mold temperature, and cooling water flow. The results served as the training dataset for machine learning modeling. The detailed information can be seen in Table S1 in Supplementary Information (SI). Four levels of heating mold temperature (T_H) were selected: 1100, 1150, 1200, and 1250 °C; four levels of drawing speed (v) were selected: 40, 60, 80, and 100 mm/min; and three levels of cooling water flow (Q) were selected: 5, 10, and 15 L/min. In addition, twenty sets of process parameters were randomly generated for finite element simulation, and the results were used as the testing dataset for machine learning modeling. The detailed information can be seen in Table S2 in SI.

2.3 Machine learning modeling

In order to predict the continuous casting process through machine learning modeling, the three-dimensional coordinate system of the Cu alloy was defined, as shown in Fig. 2. The x-axis denotes the width and extends towards the copper billet side in contact with the mold. The y-axis denotes the length and extends in the continuous casting direction. The z-axis denotes the thickness and extends towards the copper billet center. The spatial location is indicated by the three-axis coordinate system described above and defined as (x, y, z) in centimeters.

To predict the temperature at different locations, the temperatures at 1200 evenly-distributed spatial points were used for machine learning. The input variables include heating mold temperature, casting speed, cooling water flow, x, y, and z, and the output variable is the temperature at the corresponding coordinate. The temperatures at 250000 evenly-distributed spatial points were predicted by the machine learning model, and then the isotherm map could be created using Python to visualize the temperature field.

As shown in Fig. 3, to predict the location of the mushy zone, the changes in fraction solid of six lines with coordinates at (0, y_1, 0), (162.5, y_2, 0), (325, y_3, 0), (0, y_4, 9), (162.5, y_5, 9), and (325, y_6, 9) were recorded. This approach allows for determining the coordinate values of the starting and ending locations of the mushy zone under different process conditions. Points (0, y_{1M}, 0) and (0, y_{4M}, 0) were connected by a straight line, and the angle α was obtained. This enables the measurement of the inclination angle between the billet thickness direction and the solid−liquid interface when the solid fraction is 50% under varying parameters. Additionally, the average radius of cross-sectional grains in the xz-plane for various process parameters was calculated. For predicting the morphologies of mushy zones and grains, the input variables include heating mold temperature, casting speed, and cooling water flow, and the output variables are the start location (y_{1S}, y_{2S}, y_{3S}, y_{4S}, y_{5S}, y_{6S}), end location (y_{1E}, y_{2E}, y_{3E}, y_{4E}, y_{5E}, y_{6E}), inclination angle of the mushy zone, and cross-sectional grain radius.

Different algorithms were used to construct the machine learning model, including linear regression, lasso regression, support vector machine, random forest, and gradient boosting [21−23]. The finite element simulation results of sixty sets of the uniformly-distributed process conditions were used as the training dataset, and those of twenty sets of

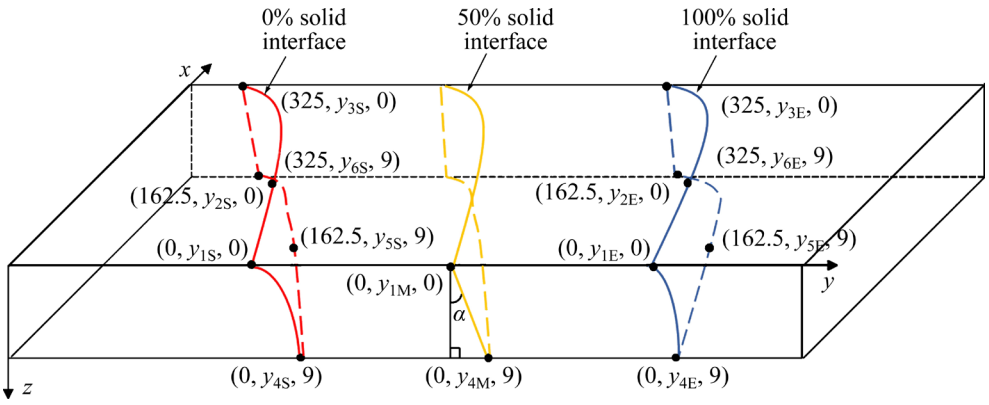

Fig. 3 Schematic diagram of measurement of mushy zone position and angle

randomly-generated process conditions were used as the testing dataset. The mean absolute percentage error (MAPE) and regression coefficient (R^2) were utilized to evaluate the accuracy of the model:

$$\mathrm{MAPE}=\frac{100\%}{n}\sum_{i=1}^{m}\left|\frac{y_i'-y_i}{y_i}\right| \tag{4}$$

$$R^2=1-\frac{\sum_{i=1}^{m}\left(y_i'-y_i\right)^2}{\sum_{i=1}^{m}\left(\overline{y}-y_i\right)^2} \tag{5}$$

where y_i is the actual value of feature i, m is the total number of features, y_i' is the prediction value of feature i, and $\overline{y}$ is the average value of y. The smaller the MAPE, the higher the R^2, and the higher the model prediction accuracy.

2.4 SHAP analysis and process parameter optimization

Based on the mapping relationship established by machine learning models, SHAP analysis was used to assess the contribution of different process parameters to the casting results. The sign (positive or negative) of the SHAP value represents the positive or negative correlation between the process parameters and the casting results, and its absolute value represents the degree of influence. SHAP values can be defined in the following way [24]:

$$\Phi_i(x)=\sum_{S\subseteq N\backslash\{i\}}\frac{|S|!(|N|-|S|-1)!}{|N|!}\left[f(x_{S\cup\{i\}})-f(x_S)\right] \tag{6}$$

where N is the total number of features, S is the subset of features without feature i, x_S denotes the portion of sample x that contains only the feature set S, $x_{S\cup\{i\}}$ denotes the portion of sample x that contains both feature i and the feature set S, and $f(x_S)$ denotes the prediction of the model in the case where only the feature set S is considered.

To ensure the surface quality of the copper plate, it is crucial for the mushy zone to be positioned between the middle of the second heat insulation section and the entrance of the cooling section [25]. Simultaneously, minimizing the inclination angle of the mushy zone is essential to promote the formation of a greater number of columnar crystals along the axial direction. The mushy zone position prediction model from the preceding section was employed to forecast the mushy zone's location for 200 sets of randomized process parameters, and the process parameters whose prediction values of y_{1S}, y_{2S}, y_{3S}, y_{1E}, y_{2E}, y_{3E} were within the range of 160−200 mm were retained. They were considered to fulfill the mushy zone position requirement. Finally, the inclination angle of the retained process parameter was predicted, and the parameter with the lowest inclination angle was used as the optimized result. The entire optimization process can be completed in 1 s to quickly obtain satisfactory process parameters.

2.5 Characterization methods

The accuracy of grain simulation was verified by examining grain morphology in industrially produced plates. The samples were cut from the longitudinal section of the alloy plates and polished, and then corroded using a solution of 2 g $FeCl_3$ + 40 mL HCl + 100 mL H_2O. Finally, microstructure observation was performed using an LV150 optical microscope and a digital camera.

3 Results and discussion

3.1 Temperature field prediction

Linear regression, lasso regression, support vector machine, random forest, and gradient boosting algorithms were used to develop prediction models for the temperature of Cu alloy at different locations. The prediction effects of different algorithms on Cu alloy temperatures are shown in Fig. 4. The random forest and gradient boosting algorithms exhibit superior MAPE and R^2, with the random forest algorithm yielding the highest performance. HCCM equipment consists of a heating section and a cooling section, which also includes a water cooling part and an air cooling part. This results in a complex nonlinear effect of process parameters on temperature distribution, making simple regression models inevitably prone to relatively high errors.

As shown in Fig. 5, the temperature distributions under two sets of process parameters from the testing set are reconstructed using the random forest model. The simulation results for the corresponding processes are also provided for comparison. It can be observed that the predicted temperature fields closely mirrored the simulated ones. The reconstructed temperature fields show similar isotherm locations and shapes as observed

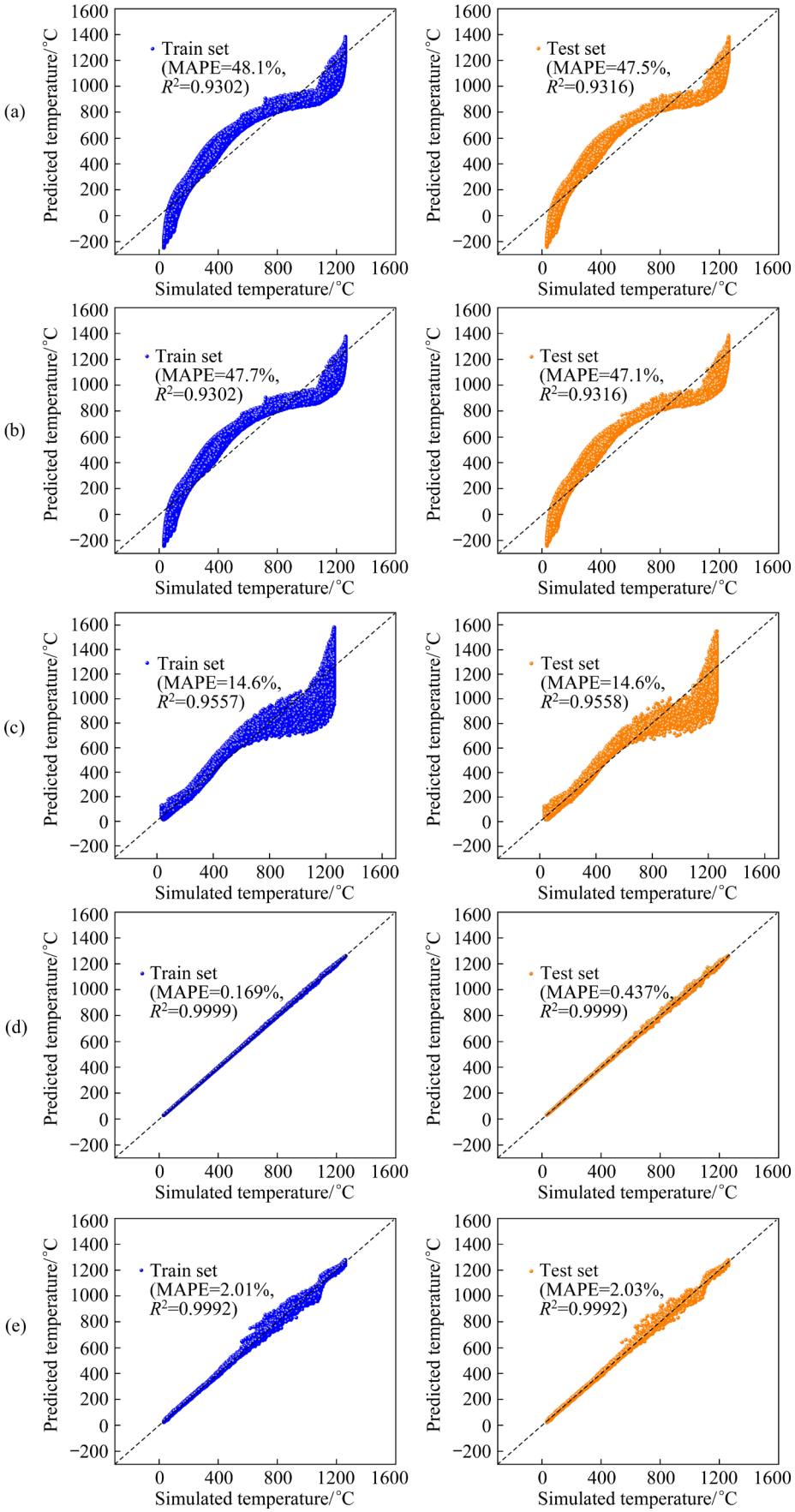

Fig. 4 Prediction effects of different algorithms on Cu alloy temperatures: (a) Linear regression; (b) Lasso regression; (c) Support vector machine; (d) Random forest; (e) Gradient boosting

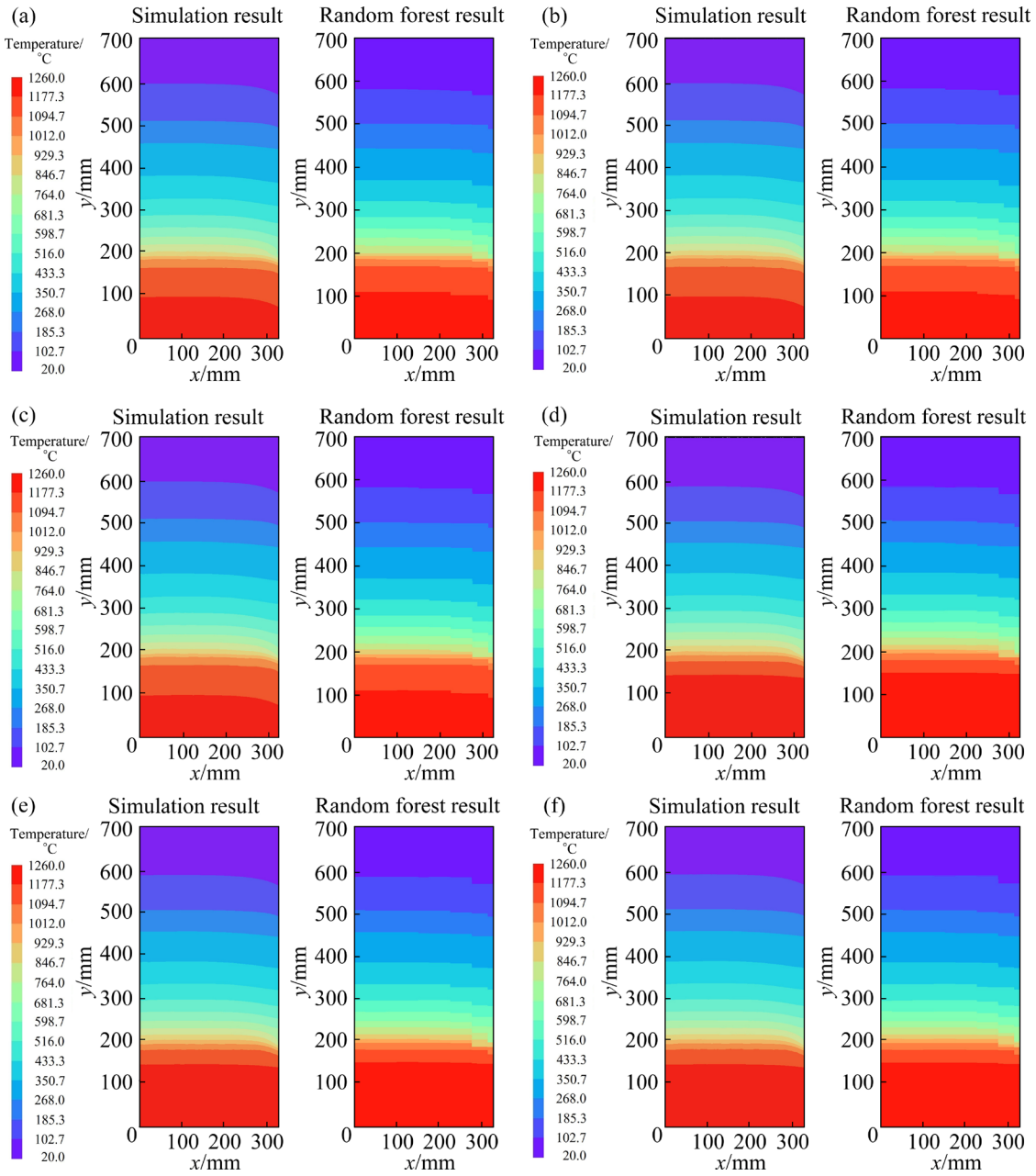

Fig. 5 Temperature fields of copper plate at different z-direction thicknesses under different process parameters: (a) 1135 °C, 65 mm/min, 15 L/min, z=0; (b) 1135 °C, 65 mm/min, 15 L/min, z=4.5 mm; (c) 1135 °C, 65 mm/min, 15 L/min, z=9 mm; (d) 1230 °C, 60 mm/min, 10 L/min, z=0; (e) 1230 °C, 60 mm/min, 10 L/min, z=4.5 mm; (f) 1230 °C, 60 mm/min, 10 L/min, z=9 mm

in the simulation results. Through the use of machine learning algorithms, the prediction model enables swift acquisition and visualization of temperature data across various process parameters and coordinates. The approach significantly reduces the time needed compared to finite element software simulations, thereby improving the efficiency in predicting the continuous casting process and offering valuable support in process control.

3.2 Mushy zone prediction

The location and shape of the mushy zone have a significant influence on the microstructure and surface quality [26]. The previously-mentioned machine learning algorithms were utilized to develop prediction models for the coordinate values from y_1 to y_6 at the start and end locations of the mushy zone, as well as the inclination angle of the mushy zone at the midpoint of the copper billet. Subsequently, the location and shape of the mushy

zone under various parameters can be estimated.

The MAPE for predicting the coordinate values from y_1 to y_6 using different algorithms on test sets is illustrated in Fig. 6. Due to the direct linear relationship between the mushy zone's location and the process parameters, support vector regression exhibits superior performance. The prediction effects of the support vector machine algorithm on all mushy zone location data are shown in Fig. 7.

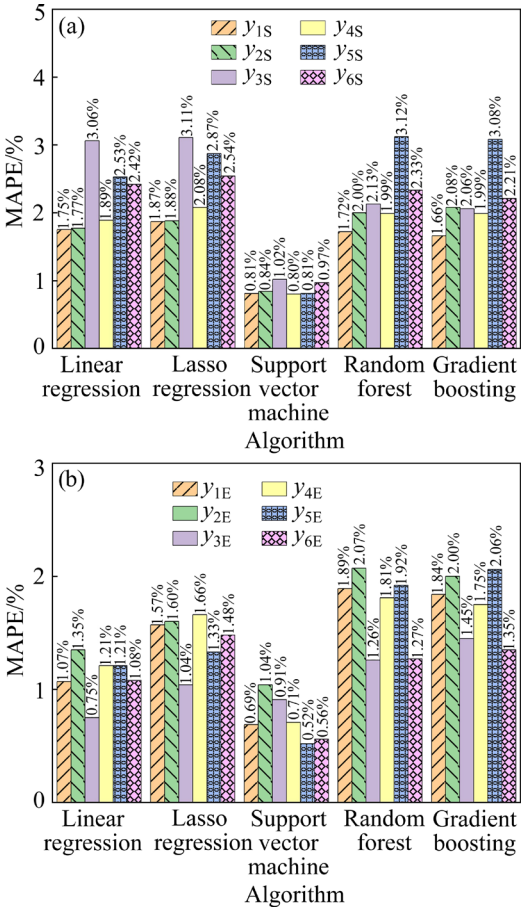

Fig. 6 MAPE values of different algorithms on predicting mushy zone locations: (a) Start location; (b) End location

The prediction effects of various algorithms on the inclination angles are shown in Fig. 8. For the integrated algorithm, the data amount was insufficient, leading to overfitting and poor training capability on the test set. Notably, the support vector machine algorithm demonstrates superior prediction performance.

3.3 Grain size prediction

Figure 9 presents a comparison of the grain morphology between the simulation and industrial

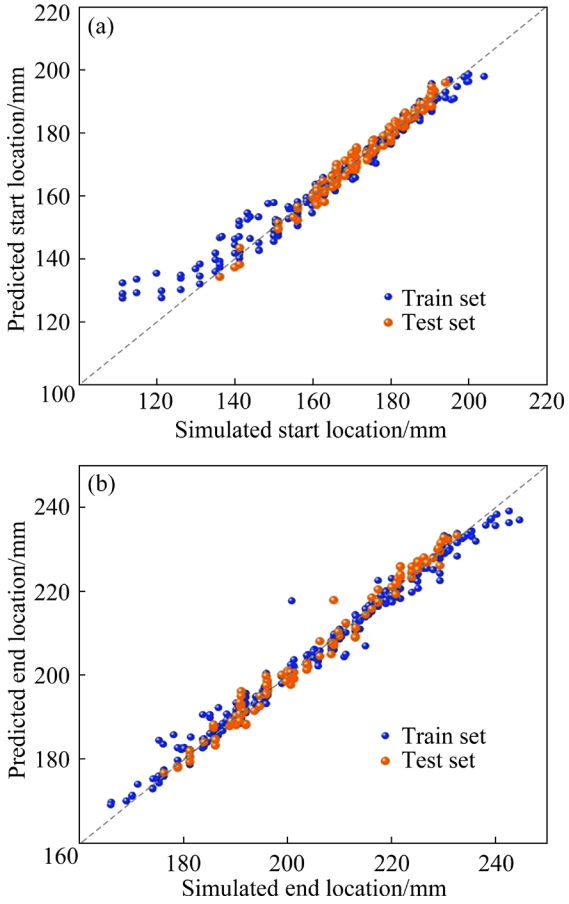

Fig. 7 Prediction effects of support vector machine on mushy zone locations: (a) Start location; (b) End location

experiment results. The present plane is in the longitudinal section at the transverse 1/2 location of the plate. The Cu alloy plate mainly consists of columnar grains. In the region close to the mold, where cooling is faster, the columnar grains are tilted, and equiaxial grains appear. The grain size decreases with increasing casting speeds due to accelerated cooling. The comparison demonstrates that the grain simulation is relatively reliable.

As shown in Fig. 10, different algorithms were used to develop prediction models for mean grain size under different process parameters. The support vector machine algorithm demonstrates superior prediction performance. For integrated algorithm, the data amount is insufficient, leading to overfitting and poor training capability on the test set.

3.4 Correlation analysis

Figure 11 illustrates the obtained SHAP values for each process parameter. The results for mushy zone location are taken as the average of the six

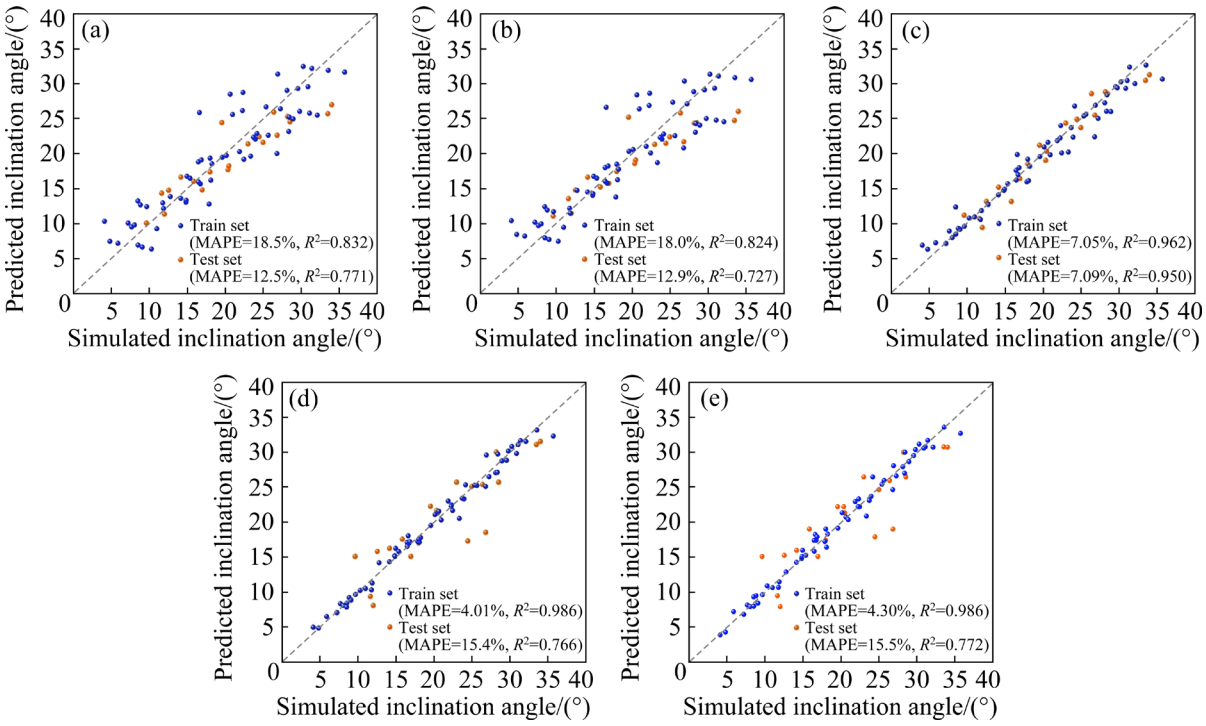

Fig. 8 Prediction effects of different algorithms on inclination angles of mushy zone: (a) Linear regression; (b) Lasso regression; (c) Support vector machine; (d) Random forest; (e) Gradient boosting

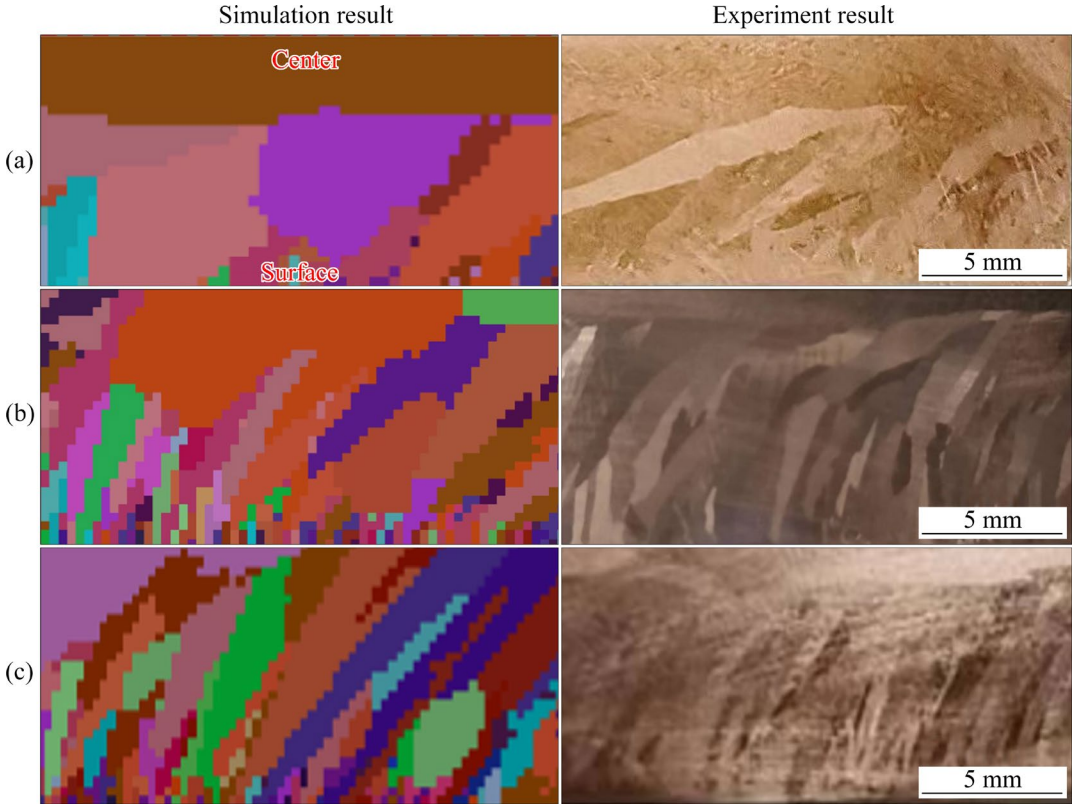

Fig. 9 Grain morphology comparison between simulation and industrial experiment results under different process parameters (heating mold temperature: 1150 °C, and cooling water flow rate: 15 L/min): (a) Casting speed of 40 mm/min; (b) Casting speed of 60 mm/min; (c) Casting speed of 100 mm/min

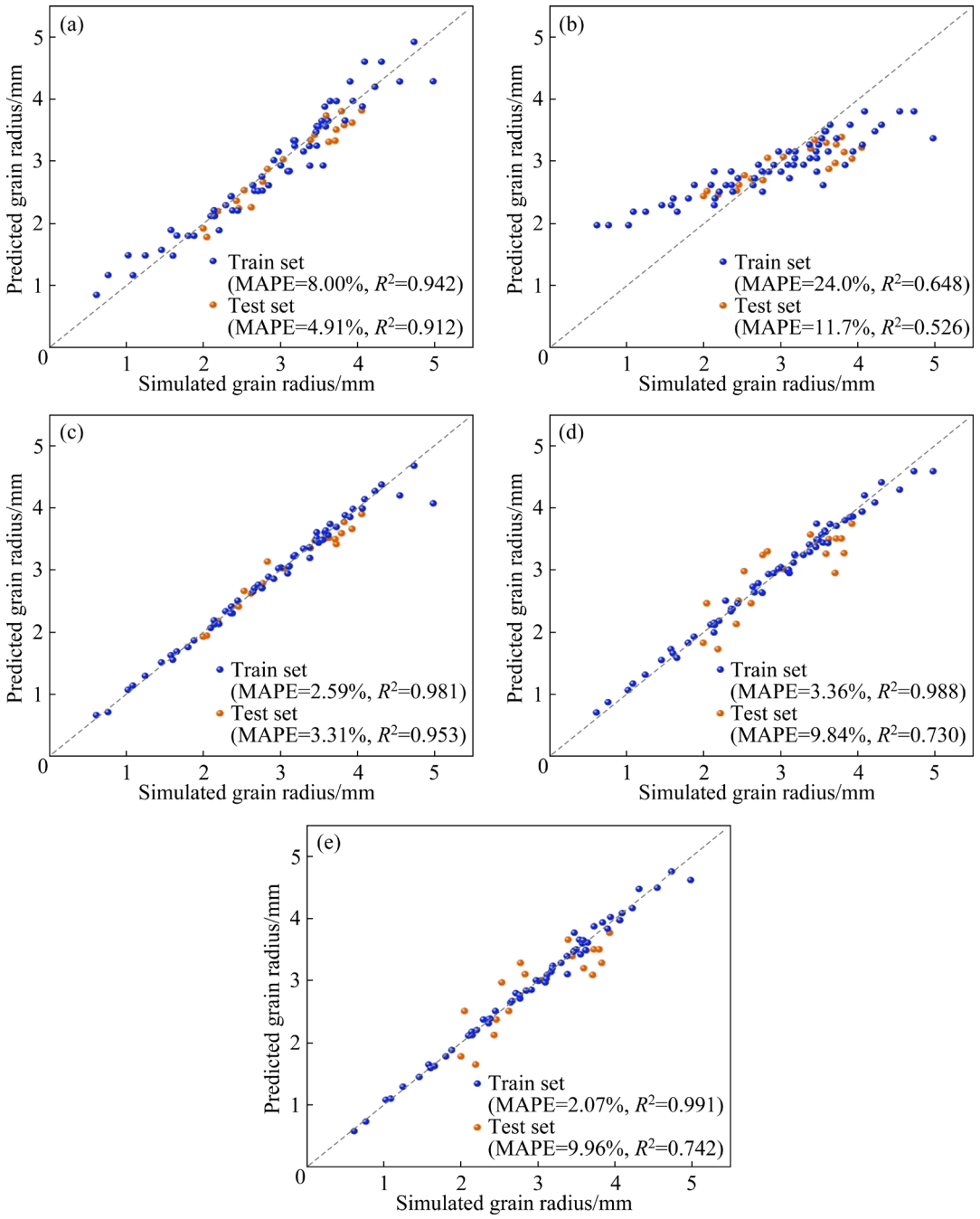

Fig. 10 Prediction effects of different algorithms on mean cross-sectional grain radius: (a) Linear regression; (b) Lasso regression; (c) Support vector machine; (d) Random forest; (e) Gradient boosting

analyzed lines. The left bar chart shows the magnitude of the impact of different process parameters on casting results. Larger mean SHAP values in the bar graph indicate that changes in this process parameter have a greater impact on the continuous casting results than others. The right summary plot illustrates how altering the parameters affects the casting results. The color of the dot indicates the value of the feature. When the horizontal coordinate moves from left to right and the value of the feature increases, it means that the result also increases as the feature value increases. Conversely, if the feature value decreases from left to right, this signifies that the result increases as the feature value decreases.

As shown in Figs. 11(a, b), the heating mold temperature has the greatest impact on the start location of the mushy zone, while the casting speed

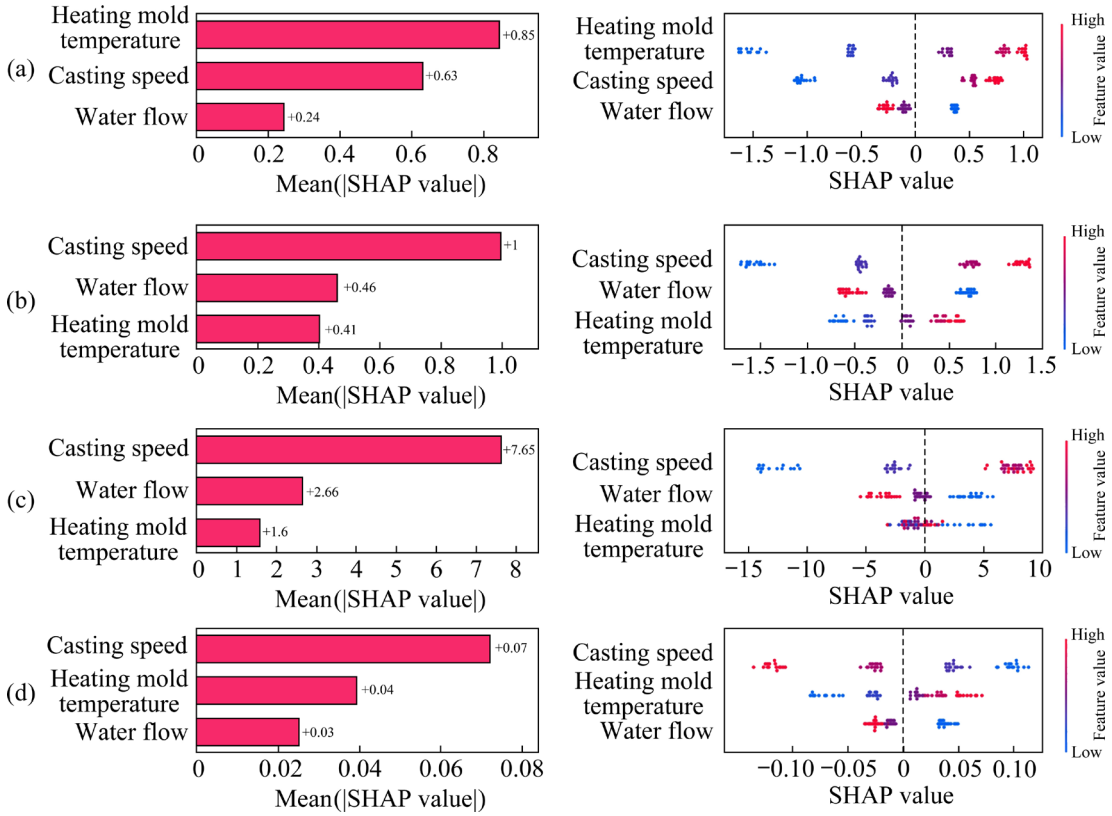

Fig. 11 SHAP value analysis of different parameters: (a) Start location of mushy zone; (b) End location of mushy zone; (c) Inclination angle of mushy zone; (d) Mean cross-sectional grain radius

primarily affects the end location of the mushy zone. With the increase in casting speed and heating mold temperature and the decrease in cooling water flow, the mushy zone moves towards the continuous casting direction. As shown in Fig. 11(c), the casting speed has the greatest impact on the inclination angle of the mushy zone. With the increase in casting speed and the decrease in cooling water flow, the inclination angle of the mushy zone increases. This phenomenon occurs because uneven cooling tends to tilt mushy zone. It is evident from Fig. 11(d) that the casting speed predominantly affects the mean cross-sectional grain radius. An increase in casting speed and cooling water flow, along with a decrease in heating mold temperature, shortens the time available for grain growth, resulting in smaller grain sizes. In conclusion, the casting speed has the greatest influence on the HCCM results and should be given priority when adjusting the process parameters. SHAP values for different parameters offer valuable insights for controlling temperature and microstructure.

3.5 Process parameters optimization

The mushy zone position is an important control target for HCCM continuous casting. As shown in Fig. 12(a), 200 lines represent 200 groups of processes, and the minimum value of y_{1S}–y_{3S} and the maximum value of y_{1E}–y_{3E} for each process are displayed, indicated by the two endpoints of line. The generated process parameters were screened to ensure that the start and end coordinates of the mushy zone were within the 160−200 mm range. The process parameters that met the requirement were highlighted in red, while those that did not were marked in black. Finally, 32 sets of process parameters were selected. Their predicted values of inclination angle are shown in Fig. 12(b), and the set of process parameters with the smallest predicted inclination angle was selected. The final optimized process parameters were as follows: heating mold temperature of 1220 °C, casting speed of 42 mm/min, and cooling water flow of 15 L/min, resulting in a mushy zone inclination angle of 6.6°. The simulation result with optimized process parameters is shown in Fig. 13. It can be observed

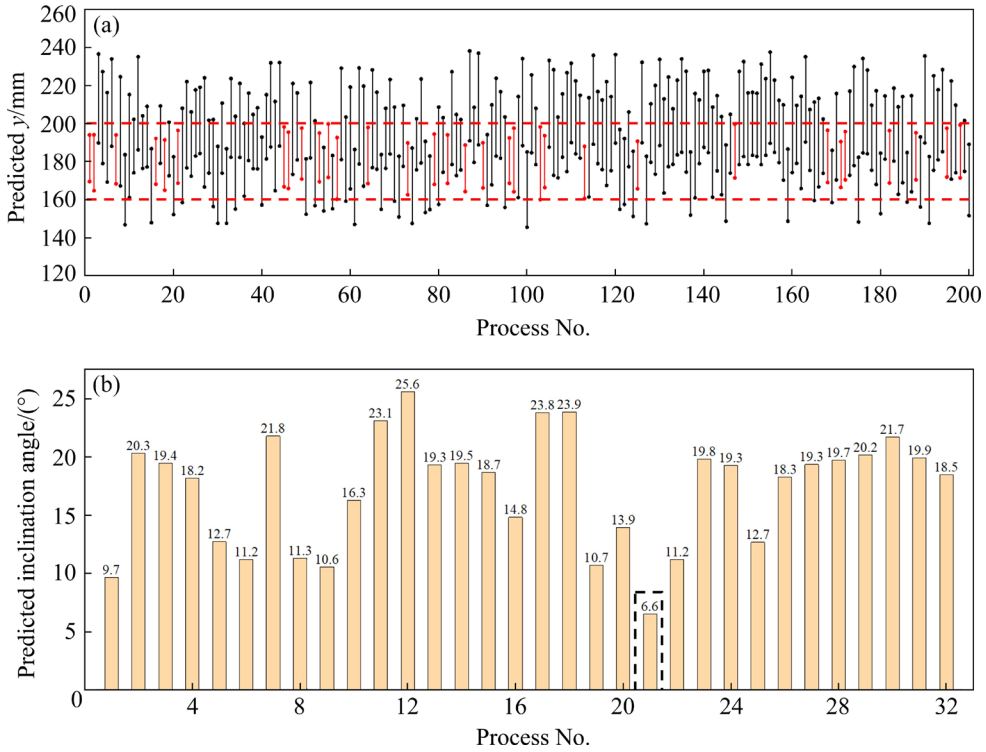

Fig. 12 Schematic diagram of optimal process selection: (a) Process parameter screening according to mushy zone prediction results; (b) Determination of optimized process parameters according to inclination angle prediction

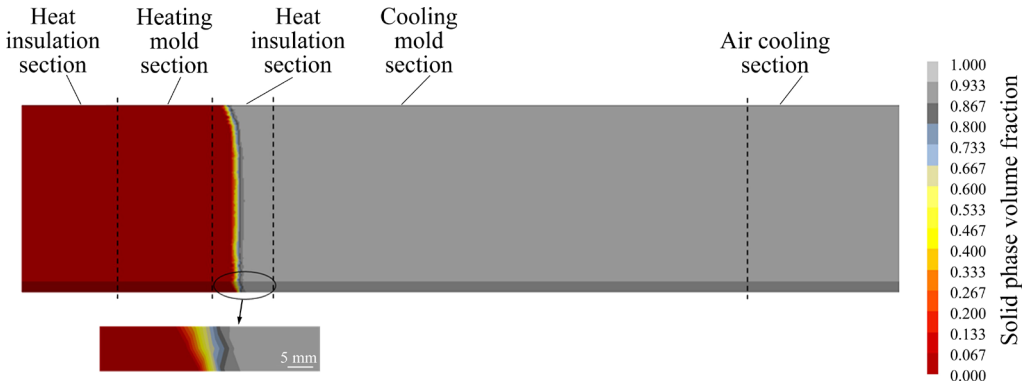

Fig. 13 Simulation results of solid phase volume fraction under optimized parameters

that the results meet the requirements of the mushy zone location and inclination angle, demonstrating the effectiveness of the optimization.

4 Conclusions

(1) The random forest algorithm outperforms others in predicting the temperature field, with errors of 0.473%. The support vector machine algorithm demonstrates superior accuracy in predicting the start and end locations of the mushy zone, with errors below 1.00%. The support vector machine algorithm also exhibits the best mushy zone inclination angle and grain size prediction accuracy, with errors of 7.09% and 3.31%, respectively.

(2) The effect of different process parameters on the HCCM results was analyzed with the help of SHAP values. The heating mold temperature exerts the most significant influence on the start location of the mushy zone. The casting speed exerts the most significant influence on the mean cross-sectional grain radius, the end location, and the inclination angle of the mushy zone, with its overall impact being the most substantial on HCCM results.

(3) HCCM process parameters were efficiently optimized in seconds with the help of the mushy

zone prediction model. The optimized parameters are: heating mold temperature of 1234 °C, casting speed of 47 mm/min, and cooling water flow rate of 10 L/min. The optimized mushy zone is located in the middle of the second heat insulation section and has an inclination angle of roughly 7°.

(4) The numerical model in this research quickly predicts and optimizes HCCM results, offering a basic method for rapid prediction and online control of the HCCM process.

CRediT authorship contribution statement

Lin-hui MENG: Conceptualization, Methodology, Data acquisition, Data analysis, Software, Writing − Original draft, Writing – Review & editing; **Fan ZHAO:** Methodology, Investigation, Formal analysis, Writing − Review & editing, Supervision; **Dong LIU:** Investigation; **Chang-jian LU:** Investigation; **Yan-bin JIANG:** Investigation, Methodology; **Xin-hua LIU:** Methodology, Writing – Review & editing, Supervision, Funding acquisition.

Declaration of competing interest

The authors declare that they have no known competing financial interests or personal relationships that could have appeared to influence the work reported in this paper.

Acknowledgments

This work was financially supported by the National Key Research and Development Program of China (No. 2023YFB3812601), the National Natural Science Foundation of China (No. 51925401) and the Young Elite Scientists Sponsorship Program by CAST, China (No. 2022QNRC001).

Supplementary Information

Supplementary Information in this paper can be found at: https://tnmsc.csu.edu.cn/download/13-p0203-2024-0518-Supplementary_Information.pdf.

References

[1] WATANABE H, KUNIMINE T, WATANABE C, MONZEN R, TODAKA Y. Tensile deformation characteristics of a Cu−Ni−Si alloy containing trace elements processed by high-pressure torsion with subsequent aging [J]. Materials Science and Engineering A, 2018, 730: 10−15.

[2] ZHAO Zhi-lei, XIAO Zhu, LI Zhou, QIU Weng-ting, JIANG Hong-yun, LEI Qian, LIU Ze-ru, JIANG Yan-bin, ZHANG Sang-jian. Microstructure and properties of a Cu−Ni−Si−Co−Cr alloy with high strength and high conductivity [J]. Materials Science and Engineering A, 2019, 759: 396−403.

[3] BAN Yi-jie, GENG Yong-feng, HOU Jin-rui, ZHANG Yi, ZHOU Meng, JIA Yan-lin, TIAN Bao-hong, LIU Yong, LI Xu, VOLINSKY A. Properties and precipitates of the high strength and electrical conductivity Cu−Ni−Co−Si−Cr alloy [J]. Journal of Materials Science & Technology, 2021, 93: 1−6.

[4] LIU Xing-jun, XIANG Shu-lin, YANG Shui-yuan, SHI Rong-pei, WANG Cui-ping. Experimental investigation of phase equilibria in the Cu−Ni−Si ternary system [J]. Journal of Alloys and Compounds, 2013, 578: 439−447.

[5] QIN Liu-xin, ZHOU Tao, JIANG Xiao-yu, WANG Meng, HU Jin-hui, WU Zi-xiao, MENG Xiang-peng, JIANG Yan-bin, LI Zhou. Microstructure and properties of Cu−Ni−Co−Si−Cr−Mg alloy by multistage thermomechanical treatment [J]. Transactions of Nonferrous Metals Society of China, 2023, 33(12): 3739−3755.

[6] LIAO Wan-neng, LIU Xue-feng, YANG Yao-hua, DU Meng. Relationship and mechanism between microstructure and property of C70250 copper alloy strip prepared by temperature controlled mold continuous casting [J]. Materials Science and Engineering A, 2019, 767: 138428.

[7] XIE Jian-xin. Development of compact processes for high efficiency fabrication of hard to working metal [J]. Materials China, 2010, 29(11): 1−7. (in Chinese)

[8] HU Jin-hui, JIANG Yan-bin, ZHAO Fan, LIU Xin-hua, LI Zhou, LU Chang-jian, LIU Ai-kui. Microstructure, properties and deformation mechanism of HCCM horizontal continuous casting Cu−Ni−Co−Si alloy strip during cold rolling [J]. Journal of Materials Research and Technology, 2023, 23: 5474−5485.

[9] JIANG Yan-bing, MAO Xiao-dong, LEI Yu, LIU Xin-hua, WANG Yi-han, XIE Jian-xin. Microstructure and mechanical property evolutions of CuNi10Fe1.8Mn1 alloy tube produced by HCCM horizontal continuous casting during drawing and its deformation mechanism [J]. Journal of Alloys and Compounds, 2019, 771: 905−913.

[10] FU Yi-lei, XIE Guo-liang, ZHAO Fan, WAN Jin-feng, MENG Xiang-hao, LIU Xiao, WANG Rui, LIU Xin-hua. Precipitation behaviors and property variations of Cu−3.0wt.%Ti fabricated by a novel short-processing non-vacuum heating-cooling combined mold continuous casting [J]. Journal of Alloys and Compounds, 2022, 921: 166059.

[11] ZHANG Hui-ran, HU Rui, LIU Xi, LI Sheng-zhou, ZHANG Guang-jie, QIAN-Quan, DING Guang-tai, DAI Dong-bo. An end-to-end machine learning framework exploring phase formation for high entropy alloys [J]. Transactions of Nonferrous Metals Society of China, 2023, 33(7): 2110−2120.

[12] LIU Chao, VENGAYIL H, LU Yu-qian, XU Xun. A Cyber-physical machine tools platform using OPC UA and MTConnect [J]. Journal of Manufacturing Systems, 2019, 51: 61−74.

[13] DONG Yi-wei, YAN Wei-guo, WU Zong-pu, ZHANG Sai-tao, LIAO Tao, YOU Yan-cheng. Modeling of shrinkage characteristics during investment casting for typical structures of hollow turbine blades [J]. International Journal

of Advanced Manufacturing Technology, 2020, 110(5−6): 1249−1260.
[14] HÜRKAMP A, OSSOWSKI T, DRÖDER K. In-mould assembly of functionally integrated structures: A surrogate model for fast quality assessment [J]. CIRP Annals, 2022, 71(1): 37−40.
[15] SUN Fei, KITA A, OGAWA T, CHEN Ta-te, ADACHI Y. Two- and three-dimensional modeling and simulations of grain growth behavior in dual-phase steel using Monte Carlo and machine learning [J]. Materials, 2023, 16(24): 7536.
[16] WANG Dong-hong, YU Jiang-ping, YANG Chang-lin, HAO Xin, ZHANG Lin, PENG Ying-hong. Dimensional control of ring-to-ring casting with a data-driven approach during investment casting [J]. The International Journal of Advanced Manufacturing Technology, 2022, 119(1): 691−704.
[17] YANG Qian-ru, LIU Qi, LIU Xin-hua, LEI Yu, JIANG Yan-bin, XIE Jian-xin, LI Zhou. Microstructure and mechanical properties of Cu−Ni−Si alloy plate produced by HCCM horizontal continuous casting [J]. Journal of Alloys and Compounds, 2022, 893: 162302.
[18] VYNNYCKY M. An asymptotic model for the formation and evolution of air gaps in vertical continuous casting [J]. Proceedings of the Royal Society A, 2009, 465(2105): 1617−1644.
[19] KOCA I. Modeling the heat flow equation with fractional-fractal differentiation [J]. Chaos, Solitons & Fractals, 2019, 128: 83−91.
[20] ZHANG Shi-jie, ZHU Bao-feng, LI Yun-bo, ZHANG Yang, LI Ri. Cellular automata-lattice Boltzmann model for polycrystalline solidification with motion of numerous dendrites [J]. Computational Materials Science, 2024, 245: 113308.
[21] CORTES C, VAPNIK V. Support-vector networks [J]. Machine Learning, 1995, 20: 273−297.
[22] BREIMAN L. Random forest [J]. Machine Learning, 2001, 45: 5−32.
[23] XIE Jian-xin, SU Yan-jing, XUE De-zhen, JIANG Xue, FU Hua-dong, HUANG Hai-you. Machine learning for materials research and development [J]. Acta Metallurgica Sinica, 2021, 57(11): 1343−1361.
[24] ALOMARI Y, ANDO M. SHAP-based insights for aerospace PHM: Temporal feature importance, dependencies, robustness, and interaction analysis [J]. Results in Engineering, 2024, 21: 101834.
[25] MEI Jun, LIU Xin-hua, JIANG Yan-bin, CHEN Song, XIE Jian-xin. Liquid-solid interface control of BFe10−1−1 cupronickel alloy tubes during HCCM horizontal continuous casting and its effect on the microstructure and properties [J]. International Journal of Minerals, Metallurgy, and Materials, 2013, 20(8): 748−758.
[26] MEI Jun, LIU Xin-hua, JIANG Yan-bin, XIE Jian-xin. Evolution of microstructure, texture and mechanical properties of BFe10−1−1 tube with microstructure along axial orientation during cold-rolling [J]. The Chinese Journal of Nonferrous Metals, 2012, 22(9): 2529−2538. (in Chinese)

C70250 合金板热冷组合铸型水平连铸过程中温度场、两相区和晶粒尺寸的快速预测数字模型

孟令辉[1,2]，赵 帆[1,2]，刘 栋[3]，鲁长建[3]，姜雁斌[4,5]，刘新华[3,6]

1. 北京科技大学 新材料技术研究院 材料先进制备技术教育部重点实验室，北京 100083；
2. 北京科技大学 新材料技术研究院 现代交通先进金属材料与加工技术北京实验室，北京 100083；
3. 河南省科学院 材料基因工程研究所，郑州 450046；
4. 中南大学 材料科学与工程学院，长沙 410083；
5. 中南大学 粉末冶金国家重点实验室，长沙 410083；
6. 北京科技大学 北京材料基因工程高精尖创新中心，北京 100083

摘 要：针对 C70250 合金板的热冷组合铸型(HCCM)水平连铸，采用机器学习辅助的方法快速准确地预测温度场、两相区和晶粒尺寸。首先，在不同工艺参数下对铸造过程进行有限元模拟，建立数据集。随后，采用不同的机器学习算法，实现对温度场、两相区位置、两相区倾斜角度和板坯晶粒尺寸的高精度预测。最后，采用随机生成、预测和筛选的策略快速优化工艺参数，从而将两相区控制在目标范围内。优化后的参数为：热型温度 1234 ℃、连铸速度 47 mm/min、冷却水流速 10 L/min。优化后的两相区位于第二隔热段的中间位置，倾斜角约为 7°。

关键词：铜合金；数值模拟；机器学习；预测模型；工艺参数优化

(Edited by Bing YANG)